

Emergence of Order in Dynamical Phases in Coupled Fractional Gauss Map

Sumit S. Pakhare^{a,*}, Varsha Daftardar-Gejji^b, Dilip S. Badwaik^a, Amey Deshpande^c, Prashant M. Gade^{d,*}

^a*Department of Physics, Kamala Nehru Mahavidyalaya, Nagpur*

^b*Department of Mathematics, Savitribai Phule Pune University, Pune*

^c*Department of Mathematics, Indian Institute of Technology, Bombay*

^d*Department of Physics, RTM Nagpur University, Nagpur*

Abstract

Dynamical behaviour of discrete dynamical systems has been investigated extensively in the past few decades. However, in several applications, long term memory plays an important role in the evolution of dynamical variables. The definition of discrete maps has recently been extended to fractional maps to model such situations. We extend this definition to a spatiotemporal system. We define a coupled map lattice on different topologies, namely, one-dimensional coupled map lattice, globally coupled system and small-world network. The spatiotemporal patterns in the fractional system are more ordered. In particular, synchronization is observed over a large parameter region. For integer order coupled map lattice in one dimension, synchronized periodic states with a period greater than one are not obtained. However, we observe synchronized periodic states with period-3 or period-6 in one dimensional coupled fractional maps even for a large lattice. With nonlocal coupling, the synchronization is reached over a larger parameter regime. In all these cases, the standard deviation decays as power-law in time with the power same as fractional-order. The physical significance of such studies is also discussed.

*Corresponding Author

Email addresses: sumitpakhare@gmail.com (Sumit S. Pakhare),
vsgejji@gmail.com (Varsha Daftardar-Gejji), badwaik_ds@rediffmail.com (Dilip S. Badwaik),
2009asdeshpande@gmail.com (Amey Deshpande),
prashant.m.gade@gmail.com (Prashant M. Gade)

Keywords: Gauss Map, Fractional calculus, Coupled map lattice
PACS: 45.10.Hj, 05.45.Ra, 05.45.Xt

1. Introduction

Discrete fractional calculus has a long history starting with Leibniz (1695) and is touched upon by almost every eminent mathematician. The recent revival of interest in fractional calculus is due to the successful application of fractional calculus in different fields such as quantum mechanics, electromagnetics, bioengineering, signal processing and many more [1, 2, 3, 4, 5, 6]. Both low-dimensional, as well as high dimensional spatiotemporal systems, are studied in this context. Fractional partial differential equations are also proposed [7, 8, 9]. In this paper, we propose a system of coupled fractional Gauss maps and study the phase transitions in it. In coupled map lattice, we study finite-dimensional difference equations coupled by Laplace operator. We generalize the difference equations to fractional-order.

Several systems in nature have inherent long term memory in it [10, 11]. Rheological systems, geophysical systems or fracture dynamics have been modelled by integrodifferential equations for a long time [12, 13, 14, 15, 16, 17]. Fractional differential equations offer an alternative modeling scheme [18, 19]. By now, we know several cases where fractional differential equations have been successful in providing a qualitative and quantitative understanding of the system [20, 21].

Fractional calculus has been successfully applied to spatiotemporal systems as well. Anomalous random walks have been observed experimentally since 1921 and several theories have been proposed to understand those. One of the recent models uses fractional diffusion equations to model it [22, 23, 24]. The fractional diffusion equations have also been useful in modelling the behaviour of random walkers in an expanding medium [25].

In compressional and shear waves in sediments, a near-linear variation of attenuation with frequency is observed over some range. The standard Biot theory predicts attenuation that increases and frequency squared or either levelling off or increasing as square root at high frequencies. An alternative theory explaining thus attenuation was proposed by Holm and Pandey. It has time-domain memory operator equivalent to a fractional derivative operator. [26]. Contribution of ions to electrical impedance in an electrolytic cell is related to the anomalous diffusion process and memory effects. Evengelista

et al proposed analytical solutions of fractional diffusion equations to explain it [27]. Decomposition of supersaturated solid solution can lead to the formation of clusters and precipitates of atoms and defects. They can change many material properties in a significant manner. Their kinetics is described by the diffusion-limited process. Sibatov and Svetukhin developed generalized equations of subdiffusion-limited growth using fractional derivatives to model this situation [28]. Another example where fractional calculus has helped to model physical phenomena is heat conduction. Classical Fourier law and heat conduction equation are inadequate for describing heat conduction in several materials. Time-nonlocal generalization using fractional calculus was proposed by Povstenko in this context[29]. Fractional calculus has also been used for spatiotemporal systems such as reaction-diffusion systems[30]. Thus fractional equations have been useful in modelling several physical systems including spatiotemporal systems.

We can construct a spatiotemporal system which comprises of units which follow fractional dynamics and such system can shed light on dynamics in several naturally occurring spatiotemporal systems.

A system consisting of two coupled fractional Henon maps was proposed in [31] and the synchronization was studied. Though coupled fractional logistic map has been studied in [32], the formulation is the same as usual coupled map lattice. The only difference is that a variant of the logistic map is used as an on-site map (see eq. 5 of [32]). Thus the entire theory of coupled map lattice can be used in this case. Our formulation has a long-term memory which is absent in standard definition of coupled map lattice. We observe that this helps in establishing long-range order even in low dimensional systems. Our definition reduces to a single fractional map in the absence of coupling. We study this formulation for a few topologies such as one-dimensional lattice, global coupling and small-world lattice. The prescription is generic enough to be extended to any underlying topology.

While fractional differential equations have been extremely successful in studies of several physical systems, their numerical simulation is tedious and time-consuming. It is easier to simulate fractional difference equations. We may be able to spot the essential characteristics of the system using such modelling. We expect a generic nature of the dynamical evolution of systems with long-term memory that can be learned using these discrete-time models. There have been very few investigations in such systems or their spatially extended counterpart. We study such systems with local as well as nonlocal coupling. Such modelling may capture some phenomena in continuous time

spatiotemporal systems with fractional-order.

From the engineering viewpoint, we note that dynamical systems with long-term memory have been studied in the context of control of chaos. So-color and co-workers [33] studied systems with extended time-delayed feedback. In this system, the evolution has a component from the feedback signal given by $(1 - R) \sum_{j=1}^t R^{j-1} x(t - j)$. Such feedback has been found extremely useful in controlling certain models as well as experimental systems. In this case, the simulation can be simplified by introducing another variable and converting it to an effectively two-dimensional system since the kernel is exponential. In our case, the kernel is a power-law and such simplification is not available. However, there have been advances in simulating electrical circuits of non-integer order and it is possible that such kernels can be experimentally realized [34].

We follow the definition in [35]. Deshpande and Daftardar-Gejji define a fractional difference operator and define the evolution as,

$$x(t) = x(0) + \frac{1}{\Gamma(\alpha)} \sum_{j=1}^t \frac{\Gamma(t - j + \alpha)}{\Gamma(t - j + 1)} [f(x(j - 1)) - x(j - 1)], \quad (1)$$

where, t is an integer, $x(0)$ is an initial condition, $0 < \alpha < 1$ and $f(x)$ is a difference equation or map. To simplify this notation, we define,

$$g_\alpha(t - j) = \frac{\Gamma(t - j + \alpha)}{\Gamma(t - j + 1)}. \quad (2)$$

Thus

$$x(t) = x(0) + \frac{1}{\Gamma(\alpha)} \sum_{j=1}^t g_\alpha(t - j) [f(x(j - 1)) - x(j - 1)], \quad (3)$$

Often-employed definition of one-dimensional coupled map lattice is following. Let $x(i, t)$ be a real variable associated with site i at time t . The evolution is usually given by,

$$x(i, t) = (1 - \epsilon) f(x(i, t - 1)) + \frac{\epsilon}{2} [f(x(i + 1, t - 1)) + f(x(i - 1, t - 1))], \quad (4)$$

where, $1 < i < N$ and ϵ is the coupling strength.

We generalize this definition and define one-dimensional coupled fractional maps in the next section. The uncoupled system evolves like N independent fractional maps, *i.e.* for $\epsilon = 0$, the evolution at each site is

described by a single fractional map. We also study synchronization and other spatiotemporal patterns in this one-dimensional locally coupled fractional maps. We extend this definition to globally coupled maps in the third section. Similar results are obtained for small-world networks. For non-local couplings, we observe synchronization over a large range of parameter space. The approach to synchronization is not exponential but a power-law. The power is found to be related to the fractional-order parameter. With local coupling, synchronized periodic states are observed. There are clear differences even in the qualitative behaviour of dynamics in presence of long-term memory.

2. Coupled fractional Gauss maps

The discrete Gauss map $f(x)$ is defined as

$$f(x) = \exp(-\nu x^2) + \beta. \quad (5)$$

We fix $\nu = -7.5$ and vary β . The discrete fractional Gauss map according to the definition in [35] is given as,

$$x(t) = x(0) + \frac{1}{\Gamma(\alpha)} \sum_{j=1}^t g_\alpha(t-j) [\exp(-7.5(x(j-1)^2)) + \beta - x(j-1)]. \quad (6)$$

Few comments are in order. Popular maps such as logistic maps or tent maps are a function of unit interval onto itself and coupled map lattice is defined in a way such that coupling keeps the range of values within the unit interval $[0,1]$. However, the fractional variant of this map does not keep the range of values in the same interval [36]. For some parameter values and initial conditions, the system blows up and values tend to infinity. We choose Gauss map since $f(x)$ is bounded for any x and is thus more stable. Apart from the Gauss map, Daftardar-Geiji and Deshpande studied Bernoulli map in their work.

We assume periodic boundary conditions and define the evolution of coupled fractional maps as,

$$x(i, t) = x(i, 0) + \frac{1}{\Gamma(\alpha)} \sum_{j=1}^t g_\alpha(t-j) G_1(x(i, j-1), x(i+1, j-1), x(i-1, j-1)) \quad (7)$$

where,

$$G_1(a, b, c) = (1 - \epsilon) f(a) + \frac{\epsilon}{2} [f(b) + f(c)] - a. \quad (8)$$

This definition matches with the extension of the fractional map to a two-dimensional Henon map [6]. For $\epsilon = 0$, the bifurcation diagram of a single fractional map is reproduced. This is a high dimensional system (even for a single map) and the attractor may depend on initial conditions. We take random initial conditions. We find that the generic nature of attractor does not change much with initial conditions as long as they are random. We note that the computations become much faster if we store values of $g_\alpha(m)$ for a given value of α for $m \leq T$ to simulate the system for T time-steps. These values of ratios of gamma functions were computed in high precision using Mathematica.

The above definition allows the possibility for the existence of a synchronized state. If $x(i, 0) = c$ for all i , the values will continue to be synchronized for all times. However, strictly speaking, synchronized fixed point or synchronized periodic state is not an absorbing state (unlike usual coupled map lattice). The future depends on all past values. So even if the values get synchronized at some time T , they need not stay synchronized since past values are different. Nonetheless, we observe spatial synchronization over a reasonable parameter range because the weight of past values reduces as a power-law. Asymptotically, we observe a state which is synchronized to an arbitrary precision.

We present results for three values of α *i.e.*, 0.4, 0.6 and 0.8. We study dynamics for various values of ϵ and β . For these maps, α is the fractional-order and ϵ is the coupling strength. We vary β between -0.40 to -0.50 which is the critical range. We consider $N = 100$ and simulate the model for 5×10^4 time steps. We use heat maps to observe and demonstrate spatiotemporal patterns in this system. The state of all the maps at every time step can be plotted with the help of heat maps. In addition to heat maps, we study spatial snapshot of the profile, time series of values of a given site, time-series of mean-field and time series of standard deviation of mean-field to learn more about dynamics.

For $\alpha = 0.4$, and $\beta = -0.40$, all the maps stay unsynchronized over the observed time. But as β approaches -0.50 the domains of almost synchronized values become bigger and bigger. These domains come back to their values after period-3. For $N = 100$, we observe an almost 3-periodic state after roughly 2×10^4 time steps. The maps change their state slightly. How-

ever, the decrease in the standard deviation of mean is a clear indicator of approach to synchronization. In Fig. 1, we show heat map for $\beta = -0.40$ and $\beta = -0.50$. It is clear as we have spatiotemporal chaos in one case while the system reaches perfect order in the second case. For visual clarity, we have plotted the heat map with only those values of $x(i, t)$ for which $\text{mod}(t, 3) = 0$. The reason is that the underlying periodicity is 3.

Same periodicity and synchronization is observed for $\alpha = 0.6$ as well. We plot heat maps of the system for two values of β , namely $\beta = -0.40$ and $\beta = -0.44$ in Fig. 2. Again, there is a clear transition from spatiotemporal chaos in one case and a synchronized state in the other. In this case, also, we have plotted heat map where the $x(i, t)$ is plotted only for $\text{mod}(t, 3) = 0$.

For $\alpha = 0.8$, the periodicity of the synchronized state changes to 6. In Fig. 3, we have shown heat map at $\beta = -0.40$ while for $\beta = -0.45$ where the $x(i, t)$ is plotted only for $\text{mod}(t, 6) = 0$. We observe a clear transition from spatiotemporal chaos in one case to a synchronized period-6 state for $\alpha = 0.8$. As the number of maps increases, time taken for synchronization increases. In Fig. 4, we have shown heat maps for systems with $N = 200$ for same parameter values.

The question is whether the synchronization can occur in the thermodynamic limit. Though we do not observe exact synchronization for period-6 states for large lattices, we believe that synchronization may occur for the period-3 state even in the thermodynamic limit. We investigate the case $\alpha = 0.6, \beta = -0.45$ and $\alpha = 0.4, \beta = -0.55$ in detail. We compute time T_N required for coupled maps to reach a state in which $\max(x(i, T_N)) - \min(x(i, T_N)) < 0.01$. We average over 20-100 configurations. The average time required T_N is plotted as a function of system size N and it shows a power-law with exponent 1.22. For $\alpha = 0.4$, the synchronization time scales with system size as a power-law again and the exponent is 0.96. It is shown in Fig. 5. (For $\alpha = 0.8$, the dynamics is multistable, some configurations reach synchronization and some do not reach synchronization. Hence we have not studied the case $\alpha = 0.8$.) It is clear that the synchronization can be achieved even in the thermodynamic limit for a period-3 state for $\alpha = 0.4$ and $\alpha = 0.6$. This is quite a unique behaviour. We have not seen reports of synchronized periodicity even for period-2 in coupled map lattice even for lattice size of 50. The reason is the following: if there is a periodicity, different sites of the CML settle down at different phases of this periodicity. Thus the spatial synchronization is not obtained with local connections alone except for synchronized fixed point [37].

In this system, the entire memory of all previous time-steps is involved in the computation. The consequence is that simulation time scales nonlinearly with time-steps. Simulating very large lattices for a very long time is not practical for this system.

Periodicity of synchronized patterns can be demonstrated by plotting the time series of an arbitrary site in time. The time series is shown in Fig. 6 for the above values of α . The dynamics is practically independent of initial conditions as long as it is random.

3. Globally Coupled Fractional Gauss Maps

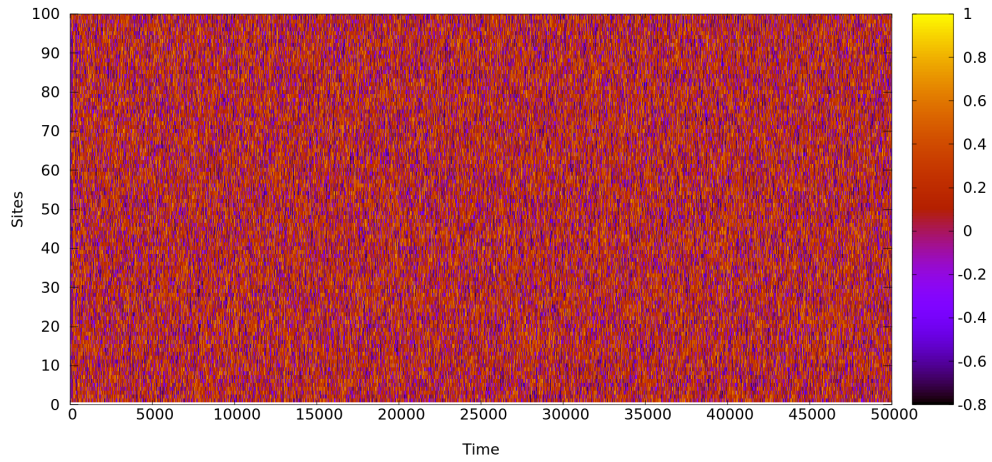
We can easily extend the above definition to the high-dimensional lattice. However, it would be cumbersome to simulate such a system and observe patterns in it. Extension of this definition to the mean-field model may shed light on behaviour in a very high dimensional system. We define globally coupled fractional map as,

$$x(i, t) = x(i, 0) + \frac{1}{\Gamma(\alpha)} \sum_{j=1}^t g_\alpha(t-j) G_2 \left(x(i, j-1), \sum_{k=1}^N f(x(k, j-1)) \right), \quad (9)$$

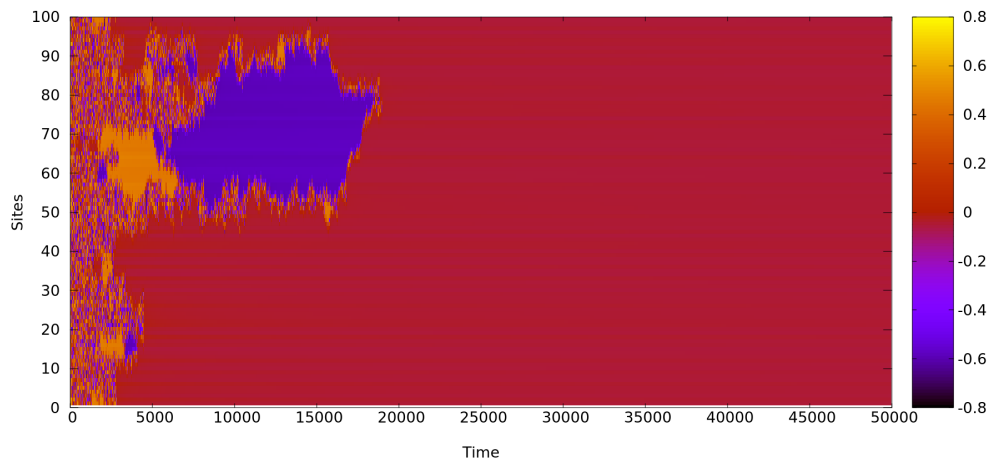
where,

$$G_2(a, b) = (1 - \epsilon)f(a) + \frac{\epsilon}{N}b - a. \quad (10)$$

We choose Gauss map as the map at a given site and vary the system parameters. We observe synchronization over a large range of parameters. The standard deviation of spatial profile system decays as a power-law in time. It goes as $t^{-\alpha}$ where α is the fractional-order parameter. For $\alpha = 0.4$ the power-law exponent is 0.4, for $\alpha = 0.6$ it is 0.6 and for $\alpha = 0.8$ it is 0.8. It is shown in Fig. 7. This nature of decay of standard deviation depends only on fractional order parameter and does not depend on other parameter values. It is superposed with oscillations if the spatially synchronized state is periodic in time. For a period-2 synchronization, the standard deviation takes smaller different values at odd and even time-steps for $\alpha = 0.6$ and $\alpha = 0.4$. These period-2 oscillations in the standard deviation for $\alpha = 0.6$ are shown in Fig. 8(a). In Fig. 8(b), we show a time series of some site. It clearly shows 2-period in time. Thus the period-2 oscillations in the standard deviation are an artefact of period-2 in synchronized phase. If we ignore the

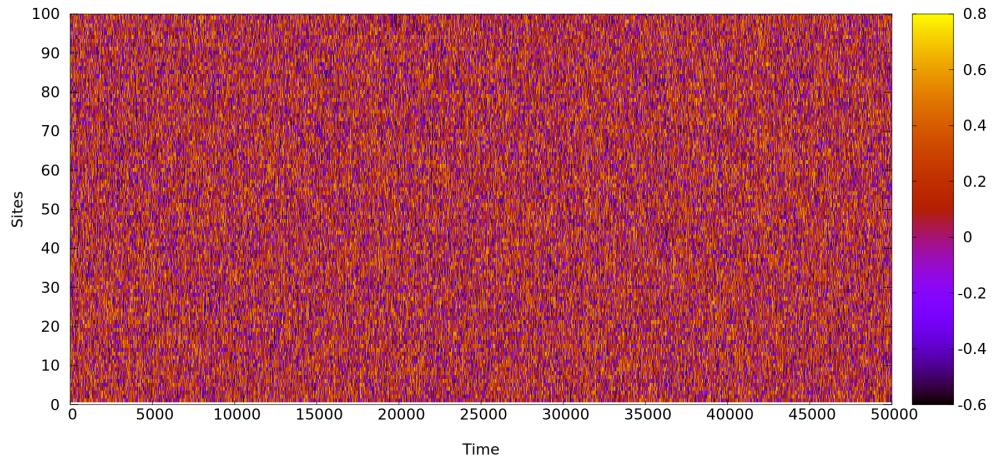


(a)

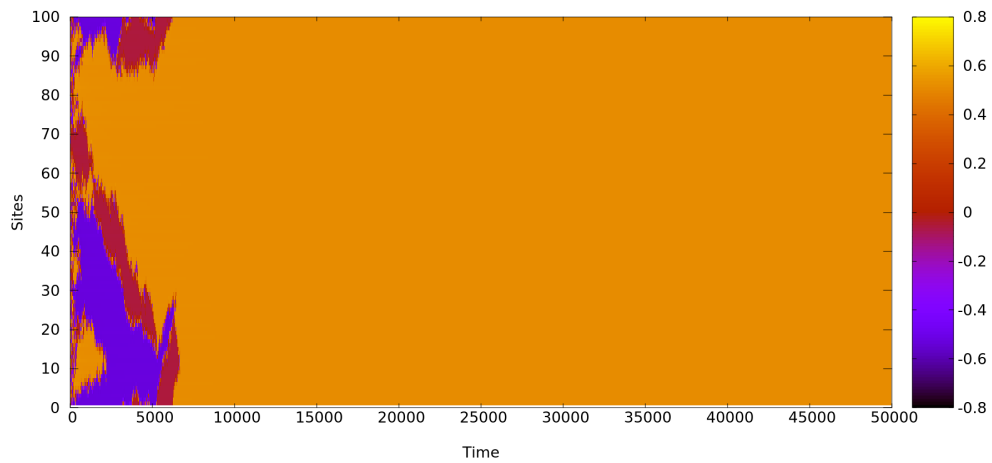


(b)

Figure 1: Heat map demonstrating spatiotemporal evolution of the system for (a) $\alpha = 0.4$ and $\beta = -0.40$ showing unsynchronized behavior for all time-steps while for (b) $\alpha = 0.4$ and $\beta = -0.50$ synchronization after 20000 time-steps is observed.

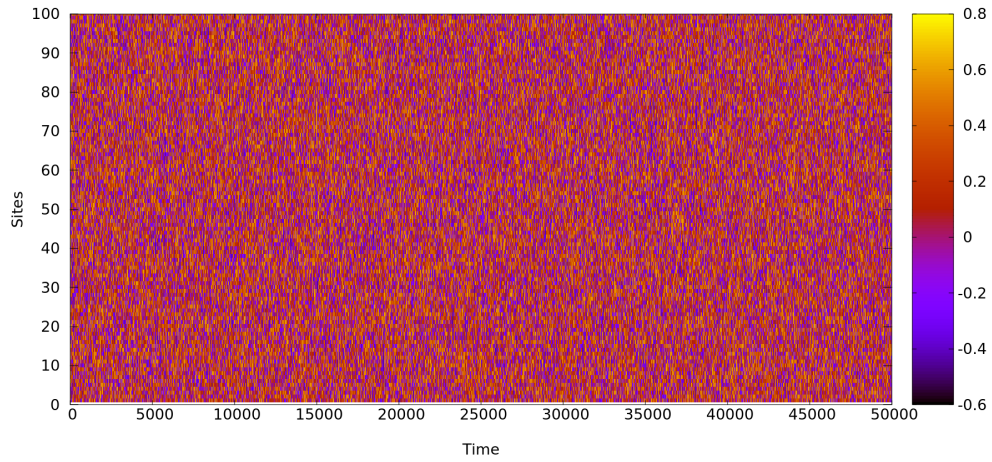


(a)

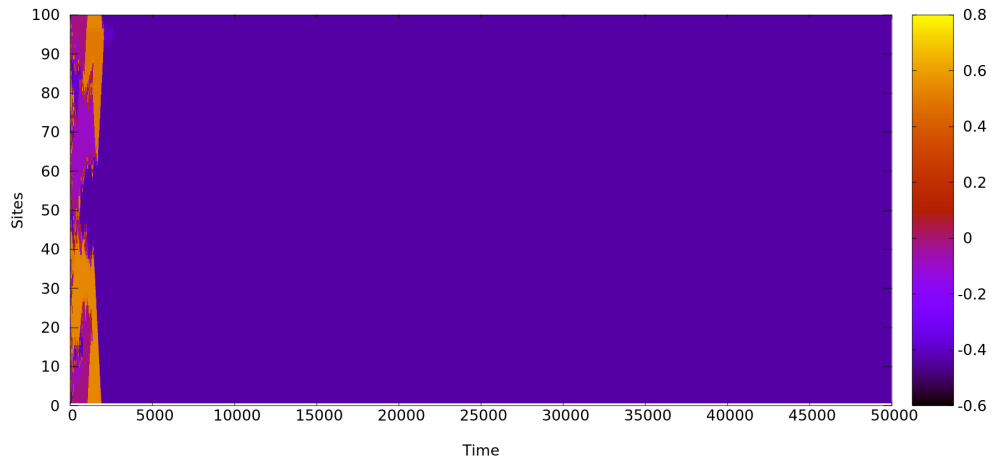


(b)

Figure 2: Heat map demonstrating spatiotemporal evolution of the system for (a) $\alpha = 0.6$ and $\beta = -0.40$, showing unsynchronized behavior for all time-steps while for (b) $\alpha = 0.6$ and $\beta = -0.44$ system synchronizes after first 7000 time steps.

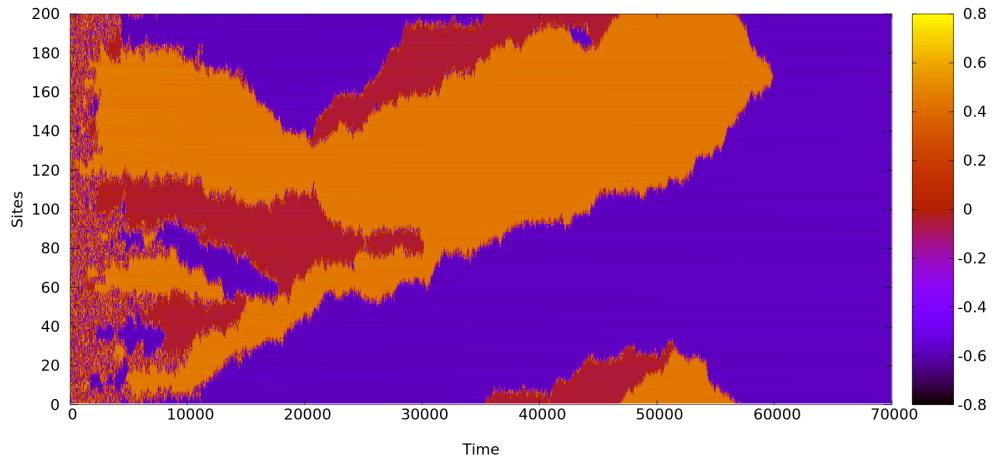


(a)

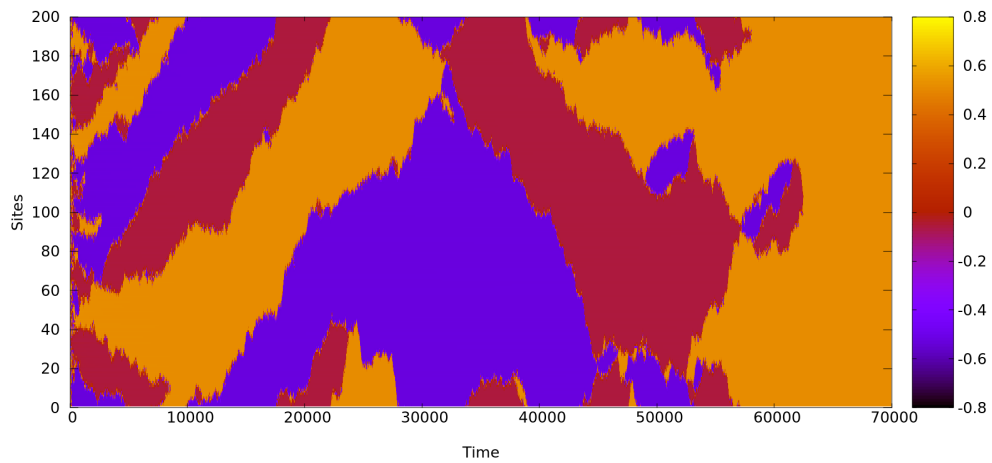


(b)

Figure 3: Heat map demonstrating spatiotemporal evolution of the system for (a) $\alpha = 0.8$ and $\beta = -0.40$ showing unsynchronized behavior for all time-steps while for (b) $\alpha = 0.8$ and $\beta = -0.45$ the system achieves synchronization early on.



(a)



(b)

Figure 4: Heat map demonstrating spatiotemporal evolution of the system for (a) $\alpha = 0.4$ and $\beta = -0.50$ (b) $\alpha = 0.6$ and $\beta = -0.44$. We simulate 200 maps and require 7×10^4 time-steps for achieving synchronization.

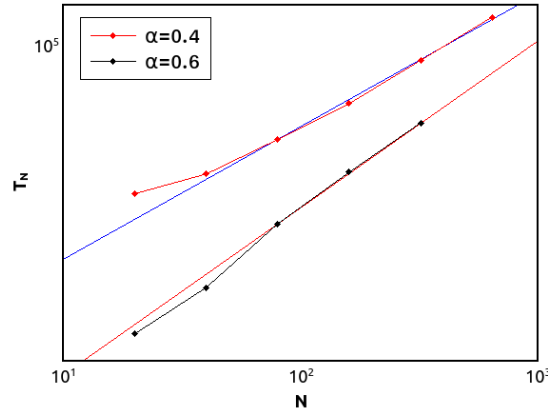


Figure 5: Average time T_N against system size N is a power-law for $\alpha = 0.4$ and $\alpha = 0.6$.

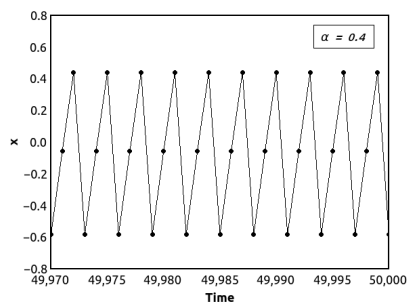
oscillations, the standard deviation decays with time as $t^{-\alpha}$. This is an expected behavior of function of Mittag-Leffler type $e_\alpha(t)$ which is related to Mittag-Leffler function as $e_\alpha(t) := E_\alpha(-t^\alpha)$ for $t > 0$. This function is important since it is an eigenfunction of the fractional relaxation equation. Mainardi [38] has shown that this function smoothly interpolates between stretched exponential function at small times and power-law decay at large times.

$$E_\alpha(-t^\alpha) = e_\alpha^0(t) = \exp\left[-\frac{t^\alpha}{\Gamma(1+\alpha)}\right], t \rightarrow 0; \quad (11)$$

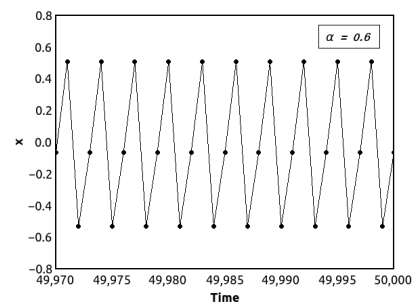
$$E_\alpha(-t^\alpha) = e_\alpha^\infty(t) = \frac{t^{-\alpha}}{\Gamma(1-\alpha)} = \frac{\sin(\alpha\pi)\Gamma(\alpha)}{\pi} \frac{1}{t^\alpha}, t \rightarrow \infty. \quad (12)$$

4. Coupled Fractional Gauss Maps with Small-World Networks

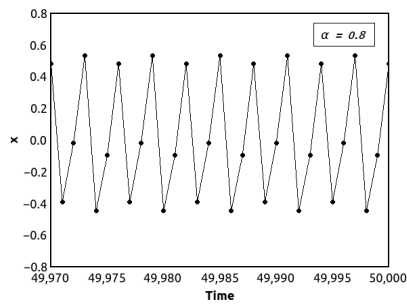
Of late, dynamics on complex networks has been extensively investigated. Most systems such as food web or internet connections do not have a topology of d -dimensional Euclidean space. Small-world, as well as scale-free networks, have been very popular models of complex networks. In small-world networks, we have a high clustering coefficient as well as small path length. We study coupled fractional maps on small-world networks. We begin with



(a)



(b)



(c)

Figure 6: Synchronization with period-3 for (a) $\alpha = 0.4$ and (b) $\alpha = 0.6$ (c) with period-6 for $\alpha = 0.8$

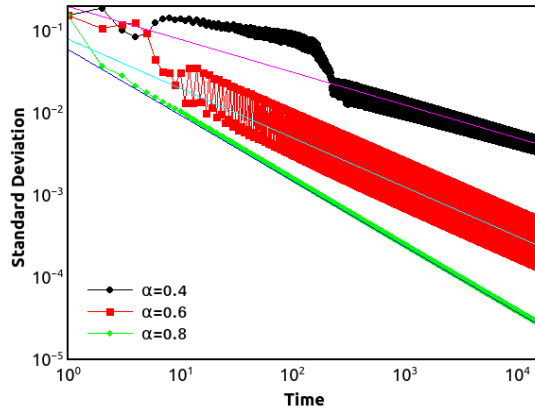
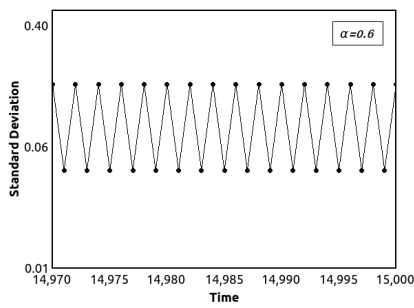
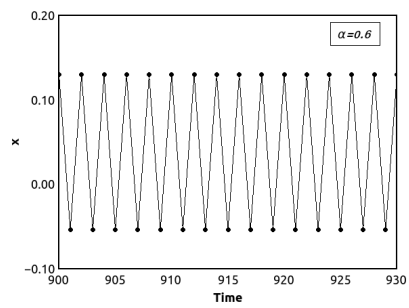


Figure 7: Power-law decay of the standard deviation in globally coupled fractional gauss maps for $\epsilon = 0.55$ and $\beta = -0.9$. For $\alpha = 0.4$ the decay exponent is 0.4. For $\alpha = 0.6$ the exponent is 0.6. For $\alpha = 0.8$ the exponent is 0.8.



(a)



(b)

Figure 8: Period-2 in globally coupled system for $\alpha = 0.6$ in (a) standard deviation (b) temporal evolution.

a one-dimensional chain where each element is coupled to two nearest neighbours on either side and replace the nearest neighbour by a randomly chosen site on the lattice with probability p . For $p = 1$, it is a network with random (undirected) neighbours which is expected to behave like a mean-field or globally coupled system. For $p = 0$, it is a simple one-dimensional chain. The small-world network allows us to interpolate between these two limits. For an equilibrium system, any value of $p > 0$ should have a behaviour similar to the mean-field model while the situation is not so clear for nonequilibrium systems. We fix $p = 0.7$ and $\beta = -0.9$, and investigate the behavior for various values of ϵ and α . The system is defined as follows,

$$x(i, t) = x(i, 0) + \frac{1}{\Gamma(\alpha)} \sum_{j=1}^t g(t-j) G_3(x(i, j-1), \sum_{k=1}^4 f(x(\xi(i, k), j-1))), \quad (13)$$

where,

$$G_3(a, b) = (1 - \epsilon)f(a) + \frac{\epsilon}{4}b - a. \quad (14)$$

We consider a system with $N = 4 \times 10^3$ sites. We simulate this system for 10^4 time steps for various values of α and ϵ . We observe that the system gets synchronized for $\epsilon = 0.8$. The standard deviation of the system decays with time as $t^{-\alpha}$ for all three values of α . This behaviour is similar to the decay in the globally coupled system discussed in the above section. For $\alpha = 0.6$ and 0.8 , and $\epsilon = 1.0$, same behavior is observed(See Fig. 9).

5. Results and Discussion

We have extended the definition of fractional maps to a coupled map lattice on arbitrary topology. The system of coupled Gauss maps is analyzed for three different values of the fractional-order parameter, α and different values of map parameter β . We have presented results for locally coupled, globally coupled and small-world networks. For locally coupled Gauss maps, we observe spatially synchronized states with period-3 or period-6 in time. Our studies indicate that such synchronization is possible even in the thermodynamic limit. For globally coupled Gauss maps, as well as for Gauss maps on a small-world network, we observe synchronization. The approach to synchronization is non-exponential over a broad range of parameters. It

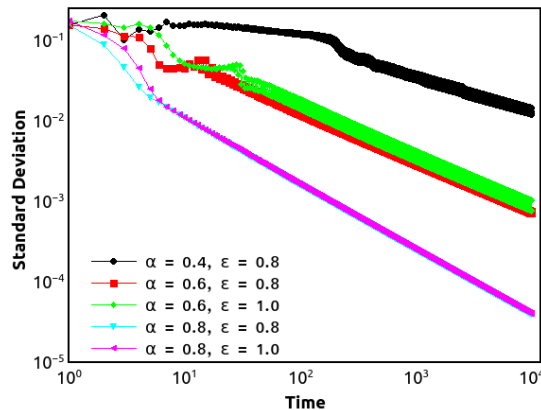


Figure 9: Power-law decay of the standard deviation in the system consisting of small-world coupled fractional Gauss maps for various values of α and ϵ . For $\alpha = 0.4$ and $\epsilon = 0.8$, the exponent is 0.4. for $\alpha = 0.6$ and $\epsilon = 0.8$, the exponent is 0.6. For $\alpha = 0.6$ and $\epsilon = 1.0$, the exponent is 0.62. For $\alpha = 0.8$ and $\epsilon = 0.8$, the exponent is 0.8. For $\alpha = 0.8$ and $\epsilon = 1.0$, the exponent is 0.8.

is a clear power-law decay. This approach is a lot slower than what is observed in integer-order systems. These results should be relevant in studies of spatially extended dynamical systems with memory. In particular, it is of interest that a) we can obtain synchronized periodic states in thermodynamic limit even with local coupling and b) approach to synchronization is a power-law with power same as the fractional order parameter. We note that for integer-order coupled map lattice, the standard deviation decays exponentially in the synchronized phase. and power-law decay is obtained only at the critical point for continuous transitions.

For globally coupled maps as well as for the small-world topology of coupled map lattices, synchronization is obtained for larger parameter values. Power-laws in space and time are observed in a range of physical phenomena and are not so common in mathematical models. A popular model for power-laws in space and time has been self-organized criticality [39]. Of late, the Griffiths phase [40] has been offered as an explanation for power-laws observed in systems such as coupled neurons. Above studies point to another possibility, namely, memory in the physical system leads to long-time dynamical correlations.

6. Acknowledgments

PMG thanks DST for financial help (EMR/2016/006685).

References

- [1] F. Atici, P. Eloe, Initial value problems in discrete fractional calculus, *Proceedings of the American Mathematical Society* 137 (3) (2009) 981–989.
- [2] H. Sheng, Y. Chen, T. Qiu, *Fractional processes and fractional-order signal processing: techniques and applications*, Springer Science & Business Media, 2011.
- [3] K. Oldham, J. Spanier, *The fractional calculus theory and applications of differentiation and integration to arbitrary order*, Vol. 111, Elsevier, 1974.
- [4] S. G. Samko, A. A. Kilbas, O. I. Marichev, et al., *Fractional integrals and derivatives*, Vol. 1993, Gordon and Breach Science Publishers, Yverdon Yverdon-les-Bains, Switzerland, 1993.
- [5] G. Z. Voyiadjis, W. Sumelka, Brain modelling in the framework of anisotropic hyperelasticity with time fractional damage evolution governed by the caputo-almeida fractional derivative, *Journal of the mechanical behavior of biomedical materials* 89 (2019) 209–216.
- [6] I. Podlubny, *Fractional differential equations*, vol. 198 of *mathematics in science and engineering* (1999).
- [7] N. Laskin, Fractional schrödinger equation, *Phys. Rev. E* 66 (2002) 056108. doi:10.1103/PhysRevE.66.056108.
URL <https://link.aps.org/doi/10.1103/PhysRevE.66.056108>
- [8] N. Laskin, *Fractional Quantum Mechanics*, WORLD SCIENTIFIC, 2018. arXiv:<https://www.worldscientific.com/doi/pdf/10.1142/10541>, doi:10.1142/10541.
URL <https://www.worldscientific.com/doi/abs/10.1142/10541>

- [9] A. Bhrawy, M. Zaky, An improved collocation method for multi-dimensional space-time variable-order fractional schrödinger equations, *Applied Numerical Mathematics* 111 (2017) 197 – 218. doi:<https://doi.org/10.1016/j.apnum.2016.09.009>. URL <http://www.sciencedirect.com/science/article/pii/S0168927416301763>
- [10] W. Sumelka, G. Z. Voyiadjis, A hyperelastic fractional damage material model with memory, *International Journal of Solids and Structures* 124 (2017) 151–160.
- [11] P. A. Nauk, [Bulletin of the Polish Academy of Sciences/Technical sciences]; *Bulletin of the Polish Academy of Sciences. Technical sciences*, PWN, 1983.
- [12] R. L. Magin, *Fractional calculus in bioengineering*, Begell House Redding, 2006.
- [13] V. Daftardar-Gejji (Ed.), *Fractional calculus: Theory and applications*, Narosa, New Delhi, 2013.
- [14] F. M. Atıcı, S. Şengül, Modeling with fractional difference equations, *Journal of Mathematical Analysis and Applications* 369 (1) (2010) 1–9.
- [15] H. Rudolf (Ed.), *Applications of fractional calculus in physics*, world scientific, 2000.
- [16] M. Klimek, Fractional sequential mechanics—models with symmetric fractional derivative, *Czechoslovak Journal of Physics* 51 (12) (2001) 1348–1354.
- [17] C. S. Drapaca, S. Sivaloganathan, A fractional model of continuum mechanics, *Journal of Elasticity* 107 (2) (2012) 105–123.
- [18] X.-J. Yang, *Advanced local fractional calculus and its applications* (2012).
- [19] R. Metzler, T. F. Nonnenmacher, Fractional relaxation processes and fractional rheological models for the description of a class of viscoelastic materials, *International Journal of Plasticity* 19 (7) (2003) 941–959.

- [20] V. E. Tarasov, Fractional dynamics: applications of fractional calculus to dynamics of particles, fields and media, Springer Science & Business Media, 2011.
- [21] K. Lazopoulos, Non-local continuum mechanics and fractional calculus, *Mechanics research communications* 33 (6) (2006) 753–757.
- [22] R. Metzler, J.-H. Jeon, A. G. Cherstvy, E. Barkai, Anomalous diffusion models and their properties: non-stationarity, non-ergodicity, and ageing at the centenary of single particle tracking, *Phys. Chem. Chem. Phys.* 16 (2014) 24128–24164. doi:10.1039/C4CP03465A.
- [23] R. Metzler, J. Klafter, The random walk’s guide to anomalous diffusion: a fractional dynamics approach, *Physics Reports* 339 (1) (2000) 1 – 77. doi:https://doi.org/10.1016/S0370-1573(00)00070-3. URL <http://www.sciencedirect.com/science/article/pii/S0370157300000703>
- [24] G.-C. Wu, D. Baleanu, Discrete chaos in fractional delayed logistic maps, *Nonlinear Dynamics* 80 (4) (2015) 1697–1703. doi:10.1007/s11071-014-1250-3. URL <https://doi.org/10.1007/s11071-014-1250-3>
- [25] S. Yuste, E. Abad, C. Escudero, Diffusion in an expanding medium: Fokker-planck equation, green’s function, and first-passage properties, *Physical Review E* 94 (3) (2016) 032118.
- [26] S. Holm, V. Pandey, Wave propagation in marine sediments expressed by fractional wave and diffusion equations, in: 2016 IEEE/OES China Ocean Acoustics (COA), IEEE, 2016, pp. 1–5.
- [27] L. Evangelista, E. Lenzi, G. Barbero, J. R. Macdonald, Anomalous diffusion and memory effects on the impedance spectroscopy for finite-length situations, *Journal of Physics: Condensed Matter* 23 (48) (2011) 485005.
- [28] R. Sibatov, V. Svetukhin, Fractional kinetics of subdiffusion-limited decomposition of a supersaturated solid solution, *Chaos, Solitons & Fractals* 81 (2015) 519–526.

- [29] Y. Povstenko, Fractional heat conduction in a space with a source varying harmonically in time and associated thermal stresses, *Journal of Thermal Stresses* 39 (11) (2016) 1442–1450.
- [30] K. M. Owolabi, Mathematical analysis and numerical simulation of patterns in fractional and classical reaction-diffusion systems, *Chaos, Solitons & Fractals* 93 (2016) 89–98.
- [31] Y. Liu, Chaotic synchronization between linearly coupled discrete fractional hénon maps, *Indian Journal of Physics* 90 (3) (2016) 313–317.
doi:10.1007/s12648-015-0742-4.
URL <https://doi.org/10.1007/s12648-015-0742-4>
- [32] Y.-Q. Zhang, X.-Y. Wang, L.-Y. Liu, Y. He, J. Liu, Spatiotemporal chaos of fractional order logistic equation in nonlinear coupled lattices, *Communications in Nonlinear Science and Numerical Simulation* 52 (2017) 52–61.
- [33] J. E. Socolar, D. W. Sukow, D. J. Gauthier, Stabilizing unstable periodic orbits in fast dynamical systems, *Physical Review E* 50 (4) (1994) 3245.
- [34] J. Gómez-Aguilar, Fundamental solutions to electrical circuits of non-integer order via fractional derivatives with and without singular kernels, *The European Physical Journal Plus* 133 (5) (2018) 197.
- [35] A. Deshpande, V. Daftardar-Gejji, Chaos in discrete fractional difference equations, *Pramana* 87 (4) (2016) 49.
- [36] G.-C. Wu, D. Baleanu, Discrete fractional logistic map and its chaos, *Nonlinear Dynamics* 75 (1-2) (2014) 283–287.
- [37] T. Bohr, G. Grinstein, Y. He, C. Jayaprakash, Coherence, chaos, and broken symmetry in classical, many-body dynamical systems, *Phys. Rev. Lett.* 58 (1987) 2155–2158. doi:10.1103/PhysRevLett.58.2155.
URL <https://link.aps.org/doi/10.1103/PhysRevLett.58.2155>
- [38] F. Mainardi, On some properties of the mittag-leffler function $E_\alpha(-t^\alpha)$, completely monotone for $t > 0$ with $0 < \alpha < 1$, arXiv preprint arXiv:1305.0161 (2013).

- [39] P. Bak, How nature works: the science of self-organized criticality, Springer Science & Business Media, 2013.
- [40] P. Moretti, M. A. Muñoz, Griffiths phases and the stretching of criticality in brain networks, Nature communications 4 (1) (2013) 1–10.